IEEE Access
Multidisciplinary ⋮ Rapid Review ⋮ Open Access Journal

Received September 15, 2020, accepted September 25, 2020, date of publication October 15, 2020,
date of current version October 29, 2020.

Digital Object Identifier 10.1109/ACCESS.2020.3031310

Amplitude and Phase Tuning of Microwave Signals in Magnetically Biased Permalloy Structures

MARTINO ALDRIGO[1], (Member, IEEE), ALINA CISMARU[1], MIRCEA DRAGOMAN[1], SERGIU IORDANESCU[1], (Life Member, IEEE), EMANUELA PROIETTI[2], GIOVANNI MARIA SARDI[2], (Member, IEEE), GIANCARLO BARTOLUCCI[2,3], AND ROMOLO MARCELLI[2], (Member, IEEE)

[1]National Institute for Research and Development in Microtechnologies, IMT Bucharest, 077190 Voluntari (Ilfov), Romania
[2]CNR-IMM Roma, 00133 Rome, Italy
[3]Department of Electronic Engineering, University of Roma "Tor Vergata," 00133 Rome, Italy

Corresponding author: Alina Cismaru (alina.cismaru@imt.ro)

This work was supported by the Romanian Ministry for Education and Research, Project "NUCLEU" no. 14N/2019, acronym MICRO-NANO-SIS-PLUS.

ABSTRACT In this paper, a permalloy layer has been employed in the fabrication of a coupled line electromagnetic bandgap (EMBG) device to tune both amplitude and phase. A magnetically biased microwave coplanar configuration manufactured with evaporated permalloy has been measured, and a circuit modelling has been studied to evaluate the measured effects in terms of variable attenuation and phase shift. Starting from a permalloy made by the mixture 80% nickel and 20% iron content, we fabricated an electromagnetic bandgap (EMBG) structure based on a periodic arrangement of single sections of a transmission line with variable impedance, also including a central region with coupled lines. The bandpass characteristics of the EMBG device can be tuned by changing permalloy's permeability through the application of a DC magnetic field H_0 (parallel to the plane of the structure). In particular, using a magnetic field up to 3000 Oe, it was possible to change the phase by ca. 45° and the amplitude by ca. 7 dB in the X band.

INDEX TERMS Electromagnetic devices, magnetic materials, magnetic films, magnetic properties, microwave magnetics.

I. INTRODUCTION

High-frequency sub-systems as telecom and/or satellite systems and signal tracking military systems require tunable microwave devices to track the signal frequency change. Signal routing or redundancy logic also take advantage from frequency selection and tuning. Several techniques are currently available to provide frequency tuning capabilities, including electronic control or the change of material properties when they are properly biased with an electric or a magnetic field.

Examples of devices tuned using an external bias that is able to change the material response are the ferroelectric ones [1], where electric field modifies the dielectric constant of the material used to implement a microwave filter or a phase shifter. Other examples of the same class are devices based on the magnetic properties of materials, like those using magnetic garnets and ferrites [2]–[4], even including some applications with permalloy [5]. Recently, also phase-change materials have been studied for magnetic recording as well as for signal processing [6]. It is worth noting that permalloy has been found to be an interesting material for health cure purposes, having useful properties at nano-size [7]. Other groups investigated both basic properties [8]–[12] and microwave potential applications for permalloy [13]–[15], with interesting results in many fields, including microwave signal processing. In this work, we have used permalloy, a well-known material for low frequency or DC applications, made by the mixture 80% nickel and 20% iron content. The change of the material's permeability, induced by the application of a DC magnetic field H_0, provides the tuning of the microwave response of the planar device.

The associate editor coordinating the review of this manuscript and approving it for publication was Dušan Grujić.

Permalloy typically has a face-centered cubic crystal structure with a lattice constant of approximately 0.355 nm when nickel concentration is around 80% [16] but, depending on the growth technique and annealing procedures, polycrystalline structures can also be obtained. For the above reasons, magnetic losses are related to material processing. In particular, thermal evaporation (the growth technique used in this paper) is suitable for polycrystalline films in the range up to 100 nm [17], with measured resistivity $\rho \sim 27\ \mu\Omega \cdot$ cm in the best case. By literature results using the same growth procedure and a non-optimized measurement technique, we have used an upper limit of 100 $\mu\Omega \cdot$ cm [18]. Specifically, in our configuration H_0 is parallel to the plane of the electromagnetic bandgap structure (where the easy axis for the magnetization is oriented), which is designed with a coupled line approach to provide a bandpass/bandstop response in the band 2-20 GHz, analogously to the configuration studied for bandstop configurations reported in [19]. The H_0 field was applied in the plane of the device, normal to the microwave signal propagation, to have a pure mode condition, because the RF magnetic field and the DC magnetic field are perpendicular between them.

Magnetic tuning is always required when analog signal processing is preferred with respect to a digital response and, not to be forgotten, also in several cases when power handling is required, which is typically higher compared to the performance of electrically tuned devices.

As a novel result w.r.t. previous findings, not only the frequency but also the amplitude and the phase of the microwave signal can be modified according to the change in the permeability of the material, evidencing the possibility for both analog and digital (threshold) response of the tested device, thus making possible both attenuation and phase control by means of a magnetically biased permalloy structure.

II. GENERAL PROPERTIES OF EMBG STRUCTURES AND DEVICE DESIGN

Electromagnetic bandgap (EMBG) devices are well known in literature to provide a bandgap periodic response [20]. In principle, they could be designed for exhibiting either absorption bands (bandstop) or bandpass characteristics for specific frequency ranges.

The proposed EMBG structure for microwave signal processing is based on a periodic arrangement of single sections of a transmission line with variable impedance, optionally including a central region with coupled lines [17], [21]. Specifically, using the approach in [21], a coupled line structure has been proposed, alternating sections with different characteristic impedances. Fig. 1a displays the single EMBG resonator, with evidence for the $\lambda/4$ and $\lambda/2$ sections including the impedance steps. The simulated electromagnetic structure is shown in Fig. 1b (top-view) and 1c (3D view), whereas the simulated performance of the scattering parameters S_{11} (reflection coefficient) and S_{21} (transmission coefficient) is shown in Fig. 2 (in terms of their modulus in dB). In detail, as it results from Fig. 1c, two 500-μm-long

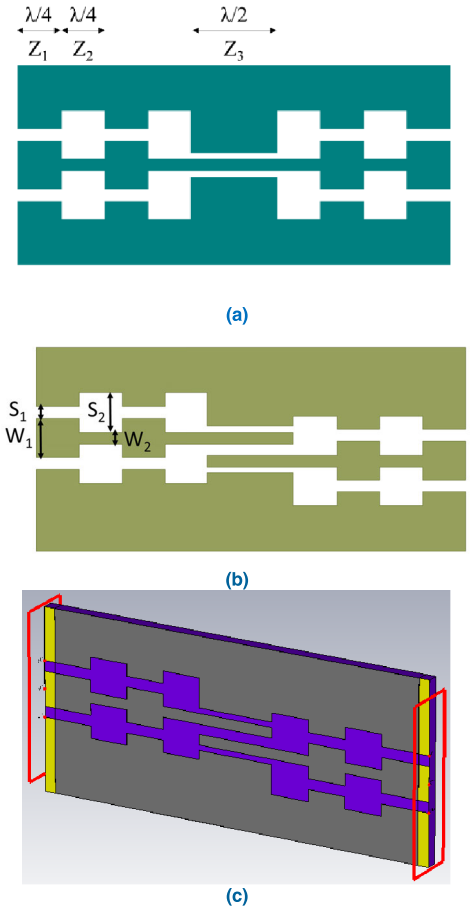

FIGURE 1. (a) Single electromagnetic bandgap (EMBG) resonator, with evidence for the $\lambda/4$ and $\lambda/2$ sections including the impedance steps; (b) EMBG structure based on coupled lines; (c) 3D EM layout of the EMBG resonator simulated in CST Microwave Studio®.

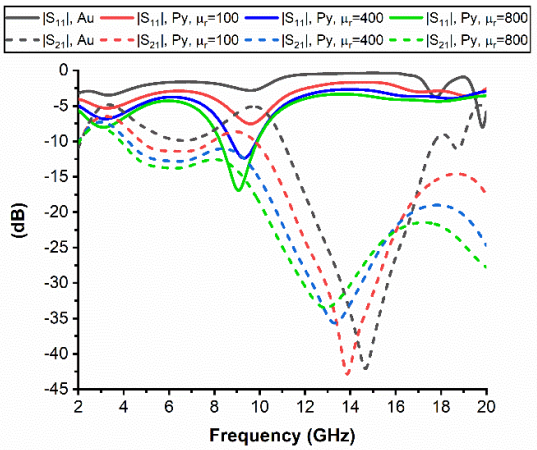

FIGURE 2. Simulated $|S_{11}|$ (solid lines) and $|S_{21}|$ (dotted lines) of the EMBG structure in the frequency range 2-20 GHz for Au and Py. Increasing values of the relative permeability (μ_r = 100, 400 and 800) have been imposed for Py.

sections of PEC (Perfect Electric Conductor) material have been added to the two excitation ports, in order to emulate the presence of the two SMA connectors used for measurements.

The simulated stack is 525-μm-thick high-resistivity silicon (HRSi), 1-μm-thick silicon dioxide (SiO_2) and 525-nm-thick permalloy (Py). The latter is modelled as a lossy conductor with conductivity 1.7×10^6 S/m and variable relative permeability $\mu_r = 100, 400, 800$. These values have been imposed starting from the unbiased material up to the magnetically saturated one. As benchmark case, the same structure has been simulated using gold (Au) instead of Py.

The input impedance of the device has been initially evaluated by means of static considerations, to get the required electrical condition when considering the two sections in cascade. Actually, the input central conductor of the first section of the coplanar waveguide has a width $W_1 = 1580$ μm and a slot $S_1 = 480$ μm, corresponding to ca. 48 Ω. The following section has $W_2 = 480$ μm and $S_2 = 1580$ μm, with a characteristic impedance of ca. 98 Ω. The central coupled-line section has a length of 3.5 mm. This choice has been inspired by the design given in [21] and properly re-scaled for working in a large frequency range up to 20 GHz. The same structure has been proposed for sensing applications in [22]. All the simulated data are re-normalized on 50 Ω, as this is the characteristic impedance of SMA connectors, as well as of the measurement setup.

Coupled lines have been used as in [22] with the goal to optimize in the next future the filtering response, after checking the material properties as a function of the DC magnetic bias. The number of cascaded cells (resonators) will be probably increased in a successive optimization, trying to find a compromise between the filter response and its size, which naturally increases because of the foot-print for each unitary cell. On the other hand, choosing different frequencies and/or alternative cells, it could be possible to maintain an acceptable size for the entire device. Presently, a simple configuration has been preferred for testing mainly the material response. According to simulations shown in Fig. 2, we can notice two main facts when using Au instead of Py: (i) three main resonances appear (around 3 GHz, 9 GHz and 20 GHz), which correspond to three maxima of S_{21}; (ii) a degradation of the bandpass behavior (as concerns S_{11}) of the EMBG structure in the frequency range 8-10 GHz can be observed. Thus, the choice of using Py appears to be a noteworthy improvement in terms of impedance matching to 50 Ω for microwave applications in the X band, which entails a better absorption of the incident signal. Additionally, the filtering characteristics of the structure change significantly when using Py, in the sense that the minimum reflection coefficient occurs at 9.1 GHz for $\mu_r = 800$. Nevertheless, increasing the value of μ_r entails an increase in filter's losses. In this respect, dielectric (HRSi, SiO_2) and magnetic (Py) materials exhibit losses which cause a degradation of the microwave signal strength inside the EMBG structure. More in detail, the dielectric losses are typically defined by means of the quantity $\tan\delta_\varepsilon$, which for permalloy are negligible w.r.t. the magnetic losses, because it is a lossy metal with magnetic properties. Actually, magnetic materials exhibit losses that are the result of intrinsic magnetic energy losses, but magnetic metals like permalloy exhibit also classical eddy-current losses, as it has been studied and measured in [23]. From the results presented in [23] and also in other literature findings, it turns out that the deposition of permalloy introduces higher losses w.r.t. those expected for a low-loss metal like gold, typically used for high-frequency devices, mainly because of the strong contribution of eddy currents. The definition of $tan\delta_\mu = \mu''/\mu'$ is often different w.r.t. the equivalent dielectric losses, which in turn are defined by $tan\delta_\varepsilon = \varepsilon''/\varepsilon'$, because for the dielectric losses we need rarely to introduce a tensor for ε; it happens only in specific cases, like for the ferroelectric materials. In the case of permalloy, and the same happens for many magnetic materials like ferrites and garnets, we have to use a tensor to describe the permeability, to include a possible anisotropic response of the material. So far, the permeability values are defined as components of a tensor describing the anisotropic behavior of a magnetic medium biased with an external magnetic field. The tensor $\boldsymbol{\mu}$ is a function of frequency, and it involves resonances owing to its derivation from the Landau-Lifschitz (LL) equation. Actually, the permeability exhibits at least one resonance frequency and, in general, a bandwidth for the existence of the modes of propagation, with frequency limits depending on the value of the external DC magnetic bias. At a given frequency, increasing the (relative) permeability value, as it has been shown in Fig. 2, higher losses are expected for the studied structure. This is also related to the combination of contributions coming from the bandpass/bandstop frequency range of the analyzed structure and the band limits imposed by the intensity of the DC external magnetic field. The equations governing the frequency response of the permeability are given by [24]:

$$\gamma_m = 1.76 \cdot 10^7 \left[\frac{rad}{Oe \cdot s}\right] \tag{1}$$

$$M_s = 10000\,[Oe] \tag{2}$$

$$\omega_m = \gamma_m M_s \tag{3}$$

$$\Delta H = 25\,[Oe] \tag{4}$$

$$\omega_{\Delta H} = \gamma_m \Delta H \tag{5}$$

$$\omega_i\,(H_0) = \gamma_m H_i\,(H_0) \tag{6}$$

$$N_{dem} = 0 \tag{7}$$

$$H_i\,(H_0) = H_0 + N_{dem} M_s \tag{8}$$

$$\alpha\,(\omega) = \frac{\gamma_m \Delta H}{2\omega} \tag{9}$$

$$\chi'_{xx}\,(\omega, H_0) = \frac{\omega_m \omega_i\,(H_0)\left(\omega_i\,(H_0)^2 - \omega^2\right) + \omega_m \omega_i\,(H_0)\,\omega^2 \alpha\,(\omega)^2}{\left(\omega_i\,(H_0)^2 - \omega^2\left(1 + \alpha\,(\omega)^2\right)\right)^2 + 4\omega_i\,(H_0)^2\,\omega^2 \alpha\,(\omega)^2} \tag{10}$$

$$\chi''_{xx}\,(\omega, H_0) = \frac{-\omega_m \omega \alpha\,(\omega)\left(\omega_i\,(H_0)^2 + \omega^2\left(1 + \alpha\,(\omega)^2\right)\right)}{\left(\omega_i\,(H_0)^2 - \omega^2\left(1 + \alpha\,(\omega)^2\right)\right)^2 + 4\omega_i\,(H_0)^2\,\omega^2 \alpha\,(\omega)^2} \tag{11}$$

$$\mu'_{xx}(\omega, H_0) = 1 + \chi'_{xx}(\omega, H_0)$$
$$\mu''_{xx}(\omega, H_0) = \chi''_{xx}(\omega, H_0) \quad (12)$$
$$tan\,\delta_{\mu}(\omega, H_0) = \frac{\mu''_{xx}(\omega, H_0)}{\mu'_{xx}(\omega, H_0)} \quad (13)$$

where γ_m is the gyromagnetic ratio, M_s is the magnetization, ω_m is the magnetization radian frequency, ΔH is the full magnetic linewidth (i.e. a measure of the magnetic losses), $\omega_{\Delta H}$ is the radian frequency associated to magnetic losses, $\omega_i(H_0)$ is the radian frequency associated to the DC magnetic bias H_0, N_{dem} is the demagnetization factor, $\alpha(\omega)$ is the frequency dependent magnetic loss, χ'_{xx} and χ''_{xx} are the real and the imaginary part of the magnetic susceptivity, μ'_{xx} and μ''_{xx} are the real and the imaginary part of the magnetic permeability, and $tan\,\delta_{\mu}$ is the magnetic loss measured by the ratio of the imaginary and real part of the magnetic permeability.

The demagnetization is zero (index N_{dem}) in the studied case of parallel DC bias and the values for the linewidth ΔH and the magnetization M_S have been chosen from literature. Anisotropy or any other additional intrinsic contribution have been neglected. Relevant parameters for the above equations are the typical values of the magnetization and the linewidth obtained for evaporated permalloy, to be used in the necessary evaluations discussed later for the magnetic losses in the exploited frequency range in Fig. 3.

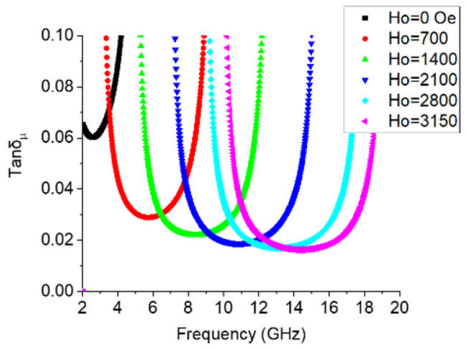

FIGURE 3. Tanδ_{μ} as a function of the frequency for increasing values of the applied external DC magnetic field.

As it is shown in Fig. 3, $tan\delta_{\mu}$ changes quickly around the band limits determined by the magnetic field H_0, and also the absolute value of the minimum is altered, with decreasing values as a function of the frequency. In this framework, to choose the value $tan\delta_{\mu} = 0.05$ for Py, is an over-estimation to justify the in-band evaluation of the EMBG structure.

The resistivity of the material, assuming a polycrystalline structure because of the used deposition technique, is quite high for thin films, as discussed also in classical literature about permalloy properties [25], [26], where both grain boundary scattering and scattering at external surfaces are occurring simultaneously. This means that a reasonable value for the permalloy resistivity in a 100 nm thick film, like the ones belonging to the multilayer grown for the purposes of this paper, is in the order of $\rho = 100\ \mu\Omega \cdot \text{cm} = 10^{-6}\Omega \cdot \text{m}$ (in agreement with the value selected for simulations).

III. TECHNOLOGY AND DEVICE MANUFACTURING

The permalloy NiFe film has been deposited by e-gun evaporation and the coupled lines EMBG structure has been manufactured by standard photolithographic mask sequence process on a 4-inch high-resistivity silicon wafer having a thickness of 525 μm.

The involved technological processes are: (1) mask manufacturing; (2) oxidation (growth of 1 μm of SiO_2 on the wafer through furnace in quartz); (3) deposition of thin films of NiFe through e-beam evaporation, base pressure 3×10^{-7} mbar, deposition rate 5 Å/s for Cr and 0.5 Å/s for Py. Actually, 5 nm of Cr are used to separate each layer of Py that is 100 nm thick, up to a total of five-layer structure; (4) lithography (Spinner-mask aligner-furnace); (5) wet chemical etching.

Five stack layers Cr/Py (5/100 nm) have been grown sequentially to maintain the same magnetic properties within the thickness [27] and to mitigate the heating effects during the deposition, thus maintaining under control the growth rate and the surface quality of the film.

The structural properties of the deposited films look like non-ideal, as already stressed in literature about the use of evaporation w.r.t. sputtering. For this reason, a polycrystalline material is presumably obtained, with losses higher than the crystalline layer obtained by means of sputtering deposition. On the other hand, the linewidth value $\Delta H = 25$ Oe can be considered in general reasonable also w.r.t. other results on permalloy obtained with sputtering, where the surface quality is higher, but leading to values for ΔH in the same order of magnitude even including the frequency dependence of the linewidth [28]. The choice for the thickness of the permalloy structure has been motivated by the necessity to decrease as much as possible the skin depth losses in metal layers, as it is usually done in the design of planar microwave devices, compatibly with the surface quality of the material deposited by evaporation, and consequently with the homogeneity of the magnetic properties along the thickness. According to literature, deposition must be under 100 nm/layer to keep the uniformity of the magnetic properties passing from one layer to the other. On the other hand, the problem is successfully solved using a multi-layer deposition (it could be by evaporation or by sputtering) with a non-magnetic metal layer at the interface. For the above reasons, a thickness around 500 nm has been chosen as a reasonable trade-off. In this framework eddy current losses are almost unavoidable. It is true, like it has been discussed in [23], that losses by eddy currents are minimized when the thickness is very small, but it is un-practical from the device design point of view. The coupled line device, cut from the silicon wafer, has been characterized using the test fixture shown in Fig. 4, in which SMA connectors of the type R125 512 000 (with central conductor for narrow strips) have been utilized to perform microwave measurements up to 20 GHz.

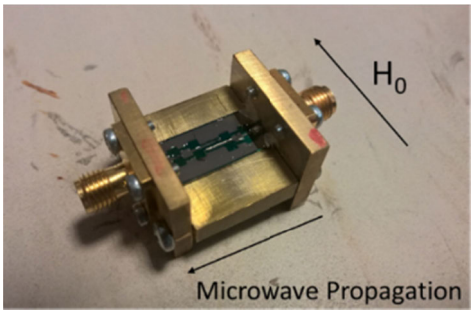

FIGURE 4. EMBG coupled line connectorized device. SMA connectors are used to connect the device in the setup. The DC magnetic bias H_0 is oriented in the device plane, perpendicular to the propagation of the microwave signal.

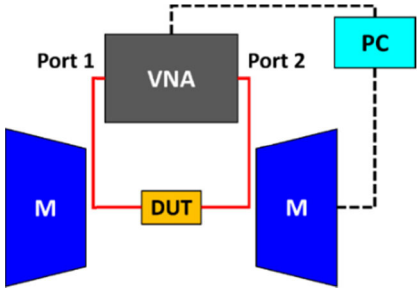

FIGURE 5. Schematic diagram of the experimental setup. The device under test (DUT) is placed between two polar expansions (M) of an electromagnet. The input/output ports of the device are connected to a two-port vector network analyzer (VNA). All the experiment is remotely controlled by a PC.

IV. CHARACTERIZATION AND DISCUSSION

The measurements have been performed by means of a two-port vector network analyzer system remotely controlled. The device has been dipped into a variable DC magnetic field provided by an electromagnet, and the magnetic field H_0 has been applied parallel to the permalloy plane, ranging between $H_0 = 0$ Oe and $H_0 = 3000$ Oe. A schematic diagram of the measurement procedure is described in Fig. 5.

The uniformity of the DC magnetic field is guaranteed within 10 Oe over an extended area, much wider than the device size, with polar expansions separated by 3 cm.

As the H_0 value is changed, the intrinsic permeability of the material is changed too, corresponding to a progressive orientation of the magnetic domains at microscopic level. At the same time, the band edges for the microwave magnetic signal are modified, in agreement with the discussion for the intrinsic losses from the previous paragraph. The experimental results recorded for the device scattering parameters are presented in Fig. 6. In detail, it can be observed that tuning the DC magnetic field H_0 allows modulating the magnitude of the reflection coefficient of the EMBG structure (Fig. 6a), keeping at the same time the bandpass behavior of the filter (Fig. 6b). The attenuation of $|S_{11}|$ due to the increase of H_0 agrees with the increase of the insertion loss for the same values of the DC magnetic field.

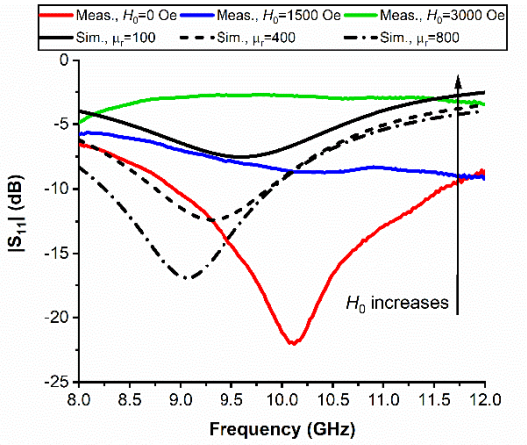

(a)

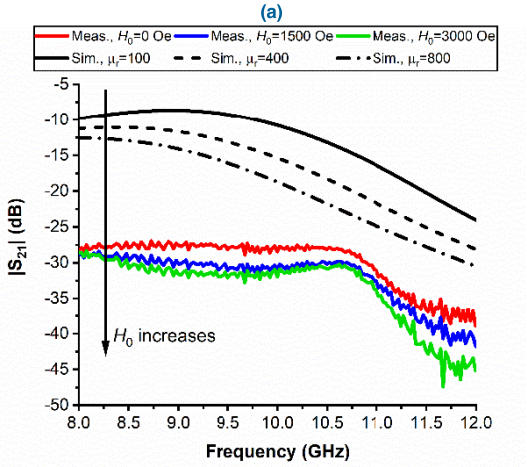

(b)

FIGURE 6. Measured and simulated scattering parameters in the X band: (a) $|S_{11}|$ and (b) $|S_{21}|$ of the EMBG structure as a function of the swept frequency, by changing the DC magnetic field/relative permeability.

Comparing the simulated results with the measured ones (Figs. 6a and 6b), it is apparent that a satisfactory agreement has been obtained in terms of both central bandpass frequency and overall bandpass behavior all over the frequency range of interest, considering that an increase of H_0 means a decrease of μ'_{xx} (see Eqs. (10) and (12)), which is related to a change of both the refraction index and the characteristic impedance of the structure at input/output ports (hence, a lower matching to the reference impedance of 50 Ω). However, some differences can be observed, as inevitably the effective refraction index n_{eff} is not the same as the simulated one, e.g. due to non-perfect Py deposition and thick SiO_2 layer. The de-tuning of the central frequency from 9.25 GHz down to 9.1 GHz is the consequence of lowering the n_{eff} of the measured prototype, which is expected if considering fabrication tolerances.

The thickness of the silicon oxide fabricated by a standard thermal oxidation process was already added in the electromagnetic simulations. On the other hand, the defects observed on the permalloy deposition are related to adhesion, with some lateral exfoliation after the photolithography and to

thickness spikes over a configuration that is, in fact, quite large. For the above reasons, we concluded that a process optimization is needed to perfectly control the deposition quality over an extended area. Presently, the structure exhibits defects that cannot be easily defined in the electromagnetic simulator, bringing to a non-negligible difference between theoretical and experimental results. Despite that, it was possible to give evidence for the basic properties of the material and its potentialities for high frequency devices. Measured losses are higher, as well, as discussed before. Nevertheless, it is worth noting that our main goal was to inspect the general properties of the material itself in processing a microwave signal for phase change and attenuation control, demanding - in future work - the use of selected area deposition in the region between the coupled lines, to fabricate similar devices with lower losses. The main reason for high insertion losses in our configuration is that the EMBG structure is wider than others used in the past for similar characterizations, bringing to device losses not acceptable for actual purposes, but improvable using additional photolithographic steps, limiting the permalloy extension to the coupling region. The measured phase change (after unwrapping the raw data to get a continuous response as a function of frequency), from the state in which the material is biased with a low DC magnetic field to the state where the material is biased with a high value of H_0, is shown in Fig. 7 for $H_0 = 0 \div 2000$ Oe.

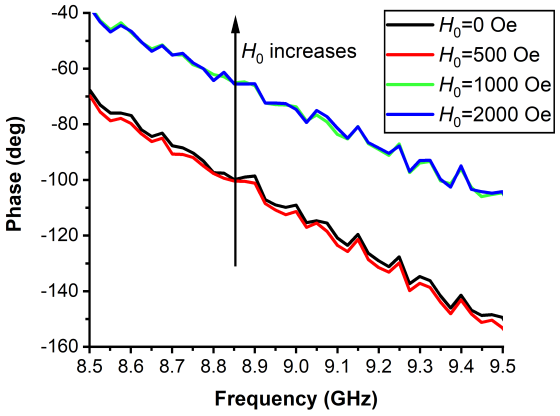

FIGURE 7. Unwrapped phase response of the EMBG structure in transmission (S_{21} parameter) in the frequency range 8.5-9.5 GHz.

As the central frequency of the EMBG structure bandpass response is around $f = 9.25$ GHz, we selected data on attenuation and phase at this frequency value to elaborate measured attenuation and phase performances.

In particular, selected data have been plotted in Fig. 8 and in Fig. 9.

Changing the permeability of permalloy, induced by the application of the DC magnetic field, the impedance of the device also changed, and the propagation of the signal too. Permalloy's permeability of the manufactured structure is lower than that of sputtered permalloy multilayers, with actual magnetic saturation around $H_0 = 1000$ Oe.

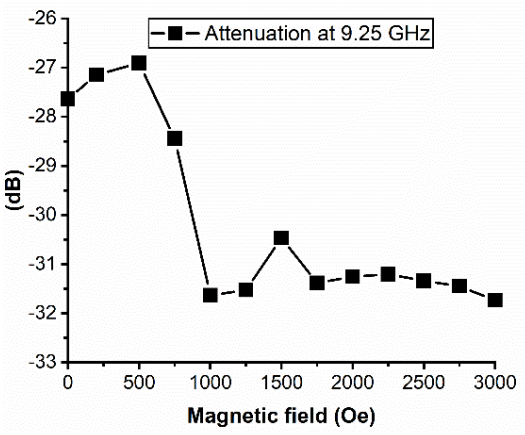

FIGURE 8. Attenuation of the structure (losses) in dB scale for different values of the applied DC magnetic field H_0 at $f = 9.25$ GHz.

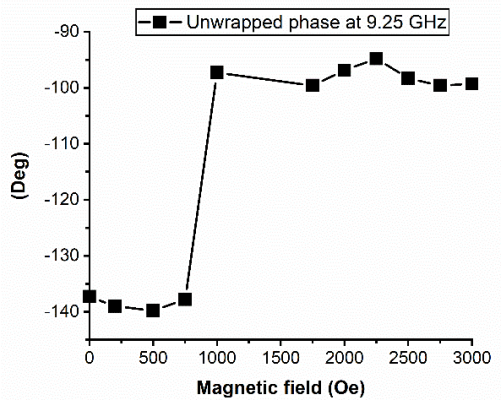

FIGURE 9. Phase change (unwrapped value) in degrees scale when increasing H_0 value at $f = 9.25$ GHz.

As a matter of fact, the transition measured around 1000 Oe has been already demonstrated in [29], where it has been discussed in detail how the magnetization is saturated depending on both: (i) the kind of substrate and (ii) the permalloy's thickness of evaporated films. In particular, the easy axis for the magnetization when permalloy is deposited onto (100)-oriented Silicon substrates lies in the plane, and the material is saturated at $H_0 = 1000$ Oe, following also the results shown in Fig. 5a of [29].

Another important consideration, introduced at the beginning of this paper, concerns with the band limitations due to the frequency range imposed by the value of the DC magnetic field H_0. Crossing the $tan\delta_\mu$ curves with the response of the EMBG structure, it is possible, within the bandpass range, to obtain higher or lower losses by properly choosing the crossover between the two curves.

It is evident, from the analysis of Fig. 6 and Fig. 7, that the linearity of the response is not always guaranteed. The response is more linear for the phase than for the amplitude, but it might also be stressed that every magnetically biased device is intrinsically non-linear, because its properties come out from the definition of the equation for the

magnetic precession and for the band limits of the magnetization response as a function of frequency. In this framework, it is worth noting that frequency tunable devices based on magnetic materials can exhibit an improved linearity using modified geometries of the ground, changing the electromagnetic boundary conditions to linearize the dispersion. It is different for the amplitude, because the squareness of the filter is always affected by a different response on the edges of the band. Nevertheless, also in this case an extension of the operational bandwidth, including cascaded structures, improves the linearity of the response at least in the center of the band, as it happens for any microwave filter.

In spite of the non-optimized device response, due to both some technology limitations and the permalloy intrinsic losses, it is evident the change in the attenuation and in the phase of the signal passing through the EMBG structure when the H_0 value has increased. As already discussed, evaporation has been demonstrated to be a difficult technique to be controlled w.r.t. other deposition techniques like sputtering and electrodeposition. This results in higher material losses, as evidenced by some difference in the magnetic linewidth at resonance. On the other hand, our results agree with typical losses mainly due to eddy currents in permalloy, which remain the most important contribution to losses expected for our structure. It is worth noting that, if permalloy is used as an absorber, or attenuator, it could be even a better result.

In particular, Fig.7 clearly exhibits a phase change with analog response of the device, i.e. a continuous change of the phase as a function of frequency. In Fig. 8 it is shown that the attenuation could also be continuously changed but the evidence for a threshold around $H_0 = 1000$ Oe favors a digital response of the structure. As a matter of fact, the analog function can be really controlled with a slow and very precise tuning around the threshold, but a digital response is clearer and less critical, especially for attenuation.

The deposition technique used to manufacture the multilayer structure usually gives back non-optimized results in terms of technology, but there are also some advantages in the easier technological process and in tailoring the properties of the structure, to have not very high values of the permeability. Actually, the response of our sample lies in the same frequency range of ferrites, but the advantage is in using a fully planar configuration with conventional photolithographic steps and with no hybrid solutions.

Using the general approach reviewed in [22] and considerations previously discussed in [30], the resonance frequency for a magnetic material biased by a DC magnetic field oriented in plane is given by the well-established equation:

$$f = \gamma \sqrt{(H_0 + H_a)\,(H_0 + H_a + 4\pi M_s)} \qquad (14)$$

Actually, the resonating frequency f is set by the material properties, including the saturation magnetization M_S, the gyromagnetic ratio γ, the anisotropy field H_a and the magnitude of an applied field H_0. For permalloy, $4\pi M_S = 10$ kG is assumed, whereas H_a is usually negligible. By imposing a DC magnetic field $H_0 = 1000$ Oe, the predicted resonance frequency is $f = 9.287$ GHz, close to the experimental center of the bandpass response, which is around 9.25 GHz. This agrees with the previous discussion, based on the cross-over between the $tan\delta_\mu$ curve and the bandpass response of the structure. Owing to the loss increase along the edges of the band limits, the attenuation is also increased, resulting in lower values for the transmission parameter S_{21}. Of course, the design of a microwave filter should be determined by electrical considerations at microwave frequencies, related to the shape and size of the sections of the planar device, and in this case the material frequency characteristics have been considered coherently with the frequency response of the studied device. The value of the permeability for comparing theoretical and experimental results can be calculated accounting for the maximum value of the susceptibility tensor component in the plane where the DC magnetic field is applied. In detail, using the classical approach developed for magnetic layers like yttrium iron garnet (YIG), the peak value of the tensorial component of the material permeability in the plane is given by $\mu''_{peak} = 4\pi M_S / \Delta H$, where ΔH is the magnetic full linewidth of the material, representing its intrinsic losses. Following the results given in classical papers about this topic for evaporated permalloy [28], [31], [32], we can assume a linewidth value for parallel resonance around $\Delta H = 25$ Oe at 9.2 GHz, leading to a permeability value of $\mu''_{peak} \approx 10000/25 = 400$.

Looking at the obtained results, the most promising effects to be pursued for the studied configuration, and to be optimized for potential next configurations, are the variable attenuation and the phase shift over extended frequency ranges, where the bandwidth depends on the filtering design at central frequencies related to the applied magnetic field and to the saturation condition for the material magnetic domains.

V. THE EQUIVALENT CIRCUIT

The aim of this section is to describe an equivalent circuit to represent permalloy component shown in Figs. 1b and 1c.

It is worth noting that the electromagnetic simulations have been performed trying to predict the expected response of the studied configuration, based on a pre-defined set of values for the permeability of permalloy, with non-negligible differences w.r.t. the experimental findings, as commented in previous sections. On the other hand, the circuit configuration presented in this section is based uniquely on the experimental results. This simple but effective approach was useful to draw additional conclusions considering the not purely resistive contribution to the device losses of the permalloy material. The circuit is developed starting from the measured results of the scattering parameters.

A. PROPOSED APPROACH FOR DERIVING THE EQUIVALENT CIRCUIT

The measured frequency behavior of $|S_{21}|$ plotted in Fig. 6 suggests to characterize the permalloy structure, at least in the frequency range 8.2-10.2 GHz and for low values of the

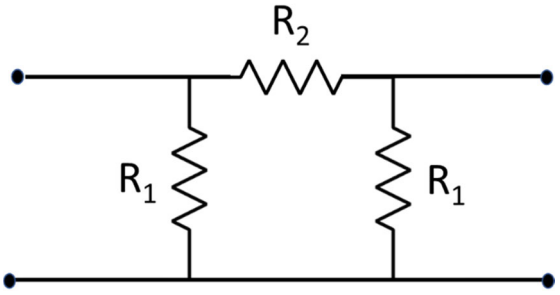

FIGURE 10. The resistive Π network modelling a microwave attenuator.

bias magnetic field H_0 ($200 \leq H_0 \leq 750$ Oe), by means of one of the models proposed in the literature for the microwave attenuators. To this end, it is here used the resistive Π network shown in Fig. 10.

Hence, the unknowns of the modeling procedure are the values of the resistors R_1 and R_2. After some algebra one obtains for R_1 and R_2:

$$R_1 = z_0 \frac{1 + |S_{11}| + |S_{21}|}{1 - |S_{11}| - |S_{21}|} \tag{15}$$

$$R_2 = \frac{z_0}{2} \frac{(1 + |S_{11}|)^2 - |S_{21}|^2}{|S_{21}|} \tag{16}$$

From Fig. 6 we can note that by increasing the magnetic bias field H_0 the scattering parameter $|S_{21}|$ cannot be considered as frequency independent even in the range 8.2-10.2 GHz. Since the equivalent circuit in Fig. 10 is composed only by resistors, it does not provide the required frequency behavior for $|S_{21}|$. In order to solve this problem, the proposed topology is modified, by inserting in the model an LC circuit, getting the configuration shown in Fig. 11.

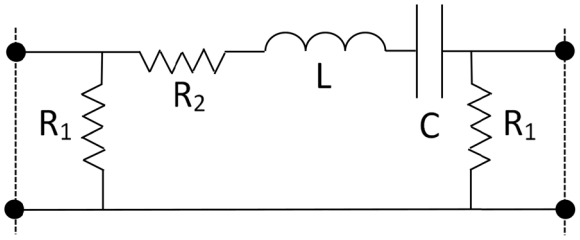

FIGURE 11. The model composed by resistors and by the LC circuit for a microwave attenuator.

The values of the inductor L and of capacitor C are obtained by using the following procedure:

- The resonant frequency f_0 of the LC circuit is chosen close to the lowest frequency value of the useful band; therefore, at f_0 the proposed circuit model is reduced to a resisitive Π network;
- R_1 and R_2 are calculated by means of (15) and (16), using for $|S_{11}|$ and $|S_{21}|$ the measured values at f_0;
- The circuit in Fig. 11 must provide, for a frequency f_1 close to the upper limit of the useful band, the corresponding measured value for $|S_{21}|$. To this end the analytic expression of S_{21} is written as follows:

$$S_{21} = \frac{1}{E + R_2 P + jXP} \tag{17}$$

where:

$$E = 1 + \frac{z_0}{R_1} \tag{18}$$

$$P = \frac{1}{2R_1}\left(2 + \frac{z_0}{R_1} + \frac{R_1}{z_0}\right) \tag{19}$$

$$X = 2\pi f L \left(1 - \frac{f_0^2}{f^2}\right) \tag{20}$$

$$f_0 = \frac{1}{2\pi\sqrt{LC}} \tag{21}$$

Imposing $f = f_1$ in (20), from (17), (18) and (19) we find:

$$L = \left[2\pi f_1 \left(1 - \frac{f_0^2}{f^2}\right)\right]^{-1} \sqrt{\frac{1}{|S_{21f_1}|^2 P^2} - \left(\frac{E}{P} + R_2\right)^2} \tag{22}$$

being S_{21f1} the measured value of S_{21} at the frequency f_1.

B. NUMERICAL RESULTS PROVIDED BY THE EQUIVALENT CIRCUIT

The above described approach has been used for modeling the permalloy structure in Fig. 1. According to the experimental behavior of $|S_{21}|$ as a function of frequency shown in Fig. 6, the values for f_0 and f_1 are so chosen respectively: $f_0 = 8$ GHz and $f_1 = 10$ GHz. For low values of the bias magnetic field H_0 two cases are analyzed: $H_0 = 200$ Oe and $H_0 = 750$ Oe. For both of them the Π configuration in Fig. 10 is used, computing the resistances R_1 and R_2 by means of (15) and (16). For high values of the bias magnetic field two cases are studied: $H_0 = 1000$ Oe and $H_0 = 3000$ Oe. The equivalent circuit for these two cases has the topology in Fig. 11, and the values of its elements are provided by the presented approach. All the obtained networks are implemented in the AWR Microwave Office software package. In Fig. 12 the $|S_{21}|$ behavior predicted by the numerical simulations is plotted as a function of frequency. These results must be compared with the measured data illustrated in Fig. 6. A good agreement can be observed in the bandwidth 8.2-10.2 GHz. Hence the effectiveness of the proposed model has been proven.

In Fig. 13, for the sake of clarity about the quality of the developed model, selected data, for $H_0 = 200$ Oe and $H_0 = 1000$ Oe, have been plotted to show the comparison between experimental and fitted data. For the phase, data have been renormalized to account for the differential phase difference.

It is important to underline that for modelling the permalloy structure we are using the equivalent circuit of an attenuator, which should essentially provide the amplitude response of

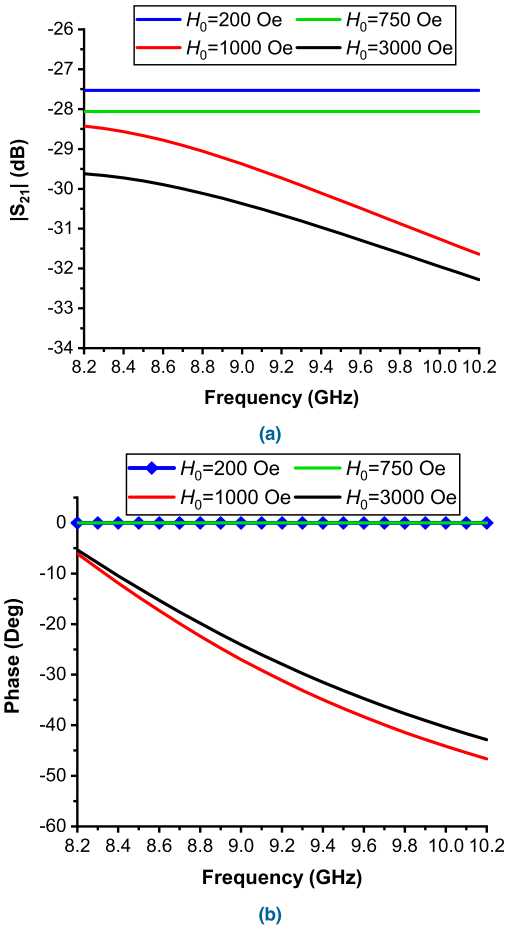

FIGURE 12. Frequency behavior for $|S_{21}|$ provided by the numerical simulations: (a) amplitude variation in dB and (b) phase shift (unwrapped) by using the magnetic field H_0 as a parameter.

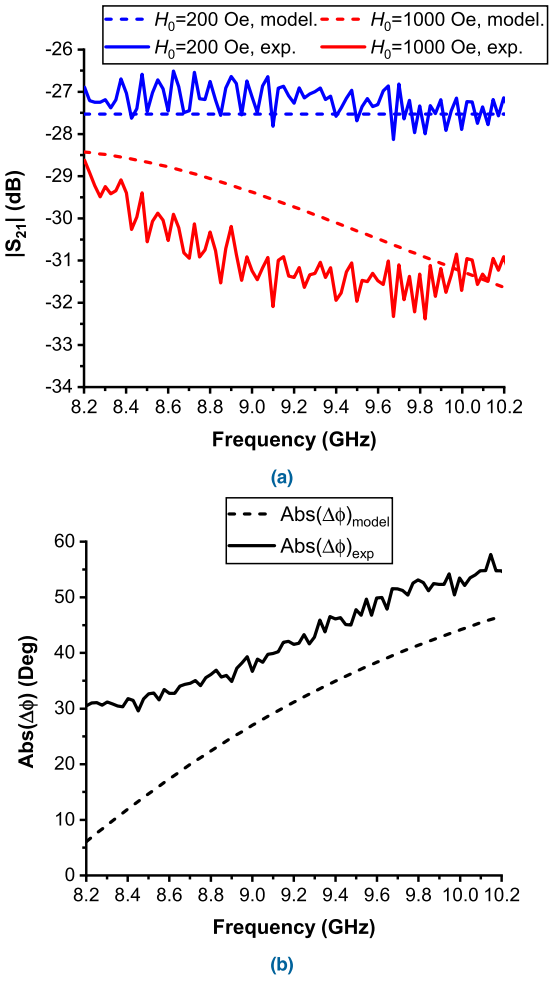

FIGURE 13. Frequency response in the X-band, centered around the central frequency of the filter (2 GHz around 9.1 GHz, with ca. 20% bandwidth) for the equivalent circuit compared with experimental results: S_{21} (a) amplitude in dB and (b) modulus of the phase difference between $H_0 = 200$ Oe and $H_0 = 1000$ Oe. Dashed lines: modelled curves. Solid lines: experimental curves.

the component. Indeed, a good agreement can be observed in Fig. 13a between simulated and measured data for $|S_{21}|$.

Even with this limitation the model gives a qualitative indication of the modulus of the phase variation due to the change in the bias magnetic field (Fig. 13b), and in particular predicts a reasonable phase change between the two states within the bandpass response.

The phase characteristics in Fig. 13b have been represented in a differential way, because what is important in a potential phase shifter is the difference in phase between the input and output ports of a device. In fact, while the equivalent circuit gives immediately the phase shift with zero reference for the input port of the device, the un-wrapped phase experimentally measured is usually affected by multiple of 2π due to the algorithm used for the un-wrapping procedure.

So far, the measured values need to be re-normalized to calculate the effective phase shift.

Actually, the level of the losses depends on the material contributions and on its magnetic bias. Nevertheless, the currently proposed circuit approach is a model using the experimental results, without having an explicit dependence of the losses from the permeability or the strength of the DC magnetic field. It might be stressed that this aspect could be an extension of the presented model, which is quantitative but not directly related to the magnetic quantities. In fact, a more elaborated equivalent circuit is under development for a full agreement between theoretical model and experiment.

As an additional and preliminary contribution to a possible full equivalent circuit, the studied configuration has been simulated with equivalent lumped elements using the circuit simulator Microwave Office. The coupling between the coplanar waveguides has been modeled by means of coupling capacitances, placed at the ends of the central device section, where the coupled lines have the geometry shown in Fig. 1b. This choice is justified by the physics of the problem, as in the equivalent circuit half of the capacitance is at the beginning of the coupling section and half of it at the end. Fitting the electromagnetic simulation with the circuital one, a quite good agreement has been obtained between the two approaches, by estimating the single coupling capacitance with a value $C_{coupl} = 20$ pF.

TABLE 1. Comparison between the phase shift performance of different configurations for magnetically tuned phase shifters.

Device	Reference	Frequency	Bandwidth	Phase Shift
Permalloy EMBG CPW coupled-lines structure	This paper	X-Band	1 GHz ca.	45° ca. at 9.25 GHz
Permalloy microstrip bandpass filter	[4]	UHF-Band	200 MHz ca.	120° ca. at 1 GHz
Fe microstrip line	[15]	C-Band	4 GHz	From 5±1° to 15±5° depending on Fe film thickness

It has been already stressed in this contribution that very few papers are available until now on the utilization of permalloy for tuning the microwave properties of devices like filters or phase shifters. Looking to current literature, the following Table 1 has been produced as a general comparison on the studied properties of permalloy in our structure.

It is clear that a full comparison among all the available data does not make sense, because device size, materials and applications are different. We selected only the phase shift, typical of the dispersion control in propagating structures. Other results are mainly focused on frequency tuning (not phase) and no contributions are available on amplitude control.

VI. CONCLUSION

In this paper, permalloy has been studied as tuning material to have a phase shift and variable attenuation over large bandwidths and has been used to fabricate a microwave planar circuit in the X band, namely an electromagnetic bandgap structure. In spite of the non-optimized filtering performances, the device clearly shows some basic characteristics related to the magnetic properties of the permalloy film, encompassing fine tuning of the output phase and variable attenuation, which in principle can be considered for both digital and analog functionalities. In detail, using a magnetic field up to 3000 Oe, it was possible to change the phase by ca. 45° and the amplitude by ca. 7 dB in the X band. Future work will be devoted to the optimization of the filtering characteristic in specific bands to be coupled with the permalloy magnetic response, to limit losses of the full device. Selective deposition techniques have to be considered for confining the lossy permalloy material in one specific area.

Variable attenuation has been considered, together with the phase change, the main characteristic response for the studied device. On the other hand, selective deposition of permalloy could be the right choice for the next implementation of the structures based on this material, to have lower losses and integrated, fully passive phase shifter applications.

The work presented in this paper is one of the few ones available in literature addressing the advantages of using a magnetic material like permalloy for tuning of the properties of a microwave device using a DC magnetically biased structure. Previous works introduced interesting applications in tunable resonating configurations and only one [4] was based on phase control of the signal. In this contribution a combined effect of insertion loss control and phase tuning has been studied with a multilayer permalloy structure.

ACKNOWLEDGMENT

The authors acknowledge the Technological Department from IMT-Bucharest for their support in manufacturing of the structures. The authors also acknowledge Giacomo Marcelli for text editing of this paper.

REFERENCES

[1] S. Gevorgian, "Ferroelectrics," in *Microwave Devices, Circuits and Systems*. London, U.K.: Springer-Verlag, 2009.
[2] V. G. Harris, "Modern microwave ferrites," *IEEE Trans. Magn.*, vol. 48, no. 3, pp. 1075–1104, Mar. 2012, doi: 10.1109/TMAG.2011.2180732.
[3] W. Palmer, D. Kirkwood, S. Gross, M. Steer, H. S. Newman, and S. Johnson, "A bright future for integrated magnetics: Magnetic components used in microwave and mm-wave systems, useful materials, and unique functionalities," *IEEE Microw. Mag.*, vol. 20, no. 6, pp. 36–50, Jun. 2019, doi: 10.1109/MMM.2019.2904381.
[4] B. A. Belyaev, K. V. Lemberg, A. M. Serzhantov, A. A. Leksikov, Y. F. Bal'va, and A. A. Leksikov, "Magnetically tunable resonant phase shifters for UHF band," *IEEE Trans. Magn.*, vol. 51, no. 6, pp. 1–5, Jun. 2015, doi: 10.1109/TMAG.2014.2368513.
[5] Z. Celinski, I. R. Harward, N. R. Anderson, and R. E. Camley, "Planar Magnetic Devices for Signal Processing in the Microwave and Millimeter Wave Frequency Range," in *Handbook of Surface Science*. Amsterdam, The Netherlands: North Holland, 2015, doi: 10.1016/B978-0-444-62634-9.00010-2.
[6] K.-C. Pan, "Vanadium dioxide based radio frequency tunable devices," Ph.D. dissertation, The Degree Doctor Philosophy Eng., School Eng., Univ. Dayton, Dayton, OH, USA, 2018. [Online]. Available: https://etd.ohiolink.edu/!etd.send_file?accession=dayton154341840843132&disposition=inline
[7] R. Ferrero, A. Manzin, G. Barrera, F. Celegato, M. Coïsson, and P. Tiberto, "Influence of shape, size and magnetostatic interactions on the hyperthermia properties of permalloy nanostructures," *Sci. Rep.*, vol. 9, no. 1, p. 6591, Dec. 2019, doi: 10.1038/s41598-019-43197-4.
[8] Y. Yin, F. Pan, M. Ahlberg, M. Ranjbar, P. Dürrenfeld, A. Houshang, M. Haidar, L. Bergqvist, Y. Zhai, R. K. Dumas, A. Delin, and J. Åkerman, "Tunable permalloy-based films for magnonic devices," *Phys. Rev. B, Condens. Matter*, vol. 92, Jul. 2015, Art. no. 024427, doi: 10.1103/PhysRevB.92.024427.
[9] H. Melikyan, A. Babajanyan, N. J. Lee, T. H. Kim, K. Lee, and B. Friedman, "Characterization of magnetoresistance hysteresis of Permalloy thin-film using near-field microwave microscope," *Thin Solid Films*, vol. 519, no. 1, pp. 399–403, 2010, doi: 10.1016/j.tsf.2010.07.024.
[10] E. V. Skorohodov, R. V. Gorev, R. R. Yakubov, E. S. Demidov, Y. V. Khivintsev, Y. A. Filimonov, and V. L. Mironov, "Ferromagnetic resonance in submicron permalloy stripes," *J. Magn. Magn. Mater.*, vol. 424, pp. 118–121, Feb. 2017, 10.1016/j.jmmm.2016.10.024.
[11] H. J. J. Liu, G. A. Riley, and K. S. Buchanan, "Directly excited backward volume spin waves in permalloy microstrips," *IEEE Magn. Lett.*, vol. 6, 2015, Art. no. 4000304, doi: 10.1109/LMAG.2015.2495162.
[12] A. Talapatra, N. Singh, and A. O. Adeyeye, "Magnetic tunability of permalloy artificial spin ice structures," *Phys. Rev. Appl.*, vol. 13, Jan. 2020, Art. no. 014034, doi: 10.1103/PhysRevApplied.13.014034.
[13] B. K. Kuanr, R. Marson, S. R. Mishra, A. V. Kuanr, R. E. Camley, and Z. J. Celinski, "Gigahertz frequency tunable noise suppressor using nickel nanorod arrays and Permalloy films," *J. Appl. Phys.*, vol. 105, no. 7, 2009, Art. no. 07A520, doi: 10.1063/1.3072824.

[14] A. Haldar and A. O. Adeyeye, "Artificial metamaterials for reprogrammable magnetic and microwave properties," *Appl. Phys. Lett.*, vol. 108, no. 2, Jan. 2016, Art. no. 022405, doi: 10.1063/1.4939852.
[15] V. Sharma, Y. Khivintsev, I. Harward, B. K. Kuanr, and Z. Celinski, "Fabrication and characterization of microwave phase shifter in microstrip geometry with Fe film as the frequency tuning element," *J. Magn. Magn. Mater.*, vol. 489, Nov. 2019, Art. no. 165412, doi: 10.1016/j.jmmm.2019.165412.
[16] R. M. Bozorth, *Ferromagnetism*. New York, NY, USA: Wiley, 1993.
[17] A. D. Avery, S. J. Mason, D. Bassett, D. Wesenberg, and B. L. Zink, "Thermal and electrical conductivity of approximately 100-nm permalloy, Ni, Co, Al, and Cu films and examination of the Wiedemann-Franz Law," *Phys. Rev. B, Condens. Matter*, vol. 92, Dec. 2015, Art. no. 214410, doi: 10.1103/PhysRevB.92.214410.
[18] B. L. Zink, A. D. Avery, R. Sultan, D. Bassett, and M. R. Pufall, "Exploring thermoelectric effects and Wiedemann–Franz violation in magnetic nanostructures via micromachined thermal platforms," *Solid State Commun.*, vol. 150, pp. 514–518, Mar. 2010, doi: 10.1016/j.ssc.2009.11.003.
[19] B. K. Kuanr, I. R. Harward, R. T. Deiotte, R. E. Camley, and Z. Celinski, "Magnetically tunable micro-strip band-stop filter: Design optimization and characterization," *J. Appl. Phys.*, vol. 97, no. 10, 2005, Art. no. 10Q103, doi: 10.1063/1.1853837.
[20] M.-S. Tong, Y. Lu, Y. Chen, M. Yang, Q. Cao, V. Krozer, and R. Vahldieck, "Design and analysis of planar printed microwave and PBG filters using an FDTD method," *Microelectron. J.*, vol. 35, no. 9, pp. 777–781, 2004, doi: 10.1016/j.mejo.2004.04.012.
[21] E. Pistono, P. Ferrari, L. Duvillaret, J.-M. Duchamp, and R. G. Harrison, "Hybrid narrow-band tunable bandpass filter based on varactor loaded electromagnetic-bandgap coplanar waveguides," *IEEE Trans. Microw. Theory Techn.*, vol. 53, no. 8, pp. 2506–2514, Aug. 2005, doi: 10.1109/TMTT.2005.852774.
[22] A. Cismaru, M. Aldrigo, C. Obreja, S. Iordanescu, and M. Dragoman, "CNT-based EMBG resonator for CO_2 gas detection," in *Proc. Symp. Design, Test, Integr. Packag. MEMS MOEMS (DTIP)*, Roma, Italy, May 2018, pp. 1–4, doi: 10.1109/DTIP.2018.8394243.
[23] C. Nistor, E. Faraggi, and J. L. Erskine, "Magnetic energy loss in permalloy thin films and microstructures," *Phys. Rev. B, Condens. Matter*, vol. 72, Jul. 2005, Art. no. 014404, doi: 10.1103/PhysRevB.72.014404.
[24] B. Lax and K. J. Button, *Microwave Ferrites and Ferrimagnetics*. New York, NY, USA: McGraw-Hill, 1962.
[25] J. C. Brice and U. Pick, "The resistivity of evaporated permalloy films," *Vacuum*, vol. 15, no. 8, pp. 409–412, 1965, doi: 10.1016/0042-207X(65)90485-9.
[26] A. F. Mayadas, J. F. Janak, and A. Gangulee, "Resistivity of Permalloy thin films," *J. Appl. Phys.*, vol. 45, no. 6, p. 2780, 1974, doi: 10.1063/1.1663668.
[27] A. A. Chlenova, A. A. Moiseev, M. S. Derevyanko, A. V. Semirov, V. N. Lepalovsky, and G. V. Kurlyandskaya, "Permalloy-based thin film structures: Magnetic properties and the giant magnetoimpedance effect in the temperature range important for biomedical applications," *Sensors*, vol. 17, no. 8, p. 1900, Aug. 2017, doi: 10.3390/s17081900.
[28] S. S. Kalarickal, P. Krivosik, M. Wu, C. E. Patton, M. L. Schneider, P. Kabos, T. J. Silva, and J. P. Nibarger, "Ferromagnetic resonance linewidth in metallic thin films: Comparison of measurement methods," *J. Appl. Phys.*, vol. 99, no. 9, 2006, Art. no. 093909, doi: 10.1063/1.2197087.
[29] A. Guittoum, A. Bourzami, A. Layadi, and G. Schmerber, "Structural, electrical and magnetic properties of evaporated permalloy thin films: Effect of substrate and thickness," *Eur. Phys. J. Appl. Phys.*, vol. 58, no. 2, p. 20301, May 2012, doi: 10.1051/epjap/2012110343.
[30] B. Kuanr, I. R. Harward, D. L. Marvin, T. Fal, R. E. Camley, D. L. Mills, and Z. Celinski, "High-frequency signal processing using ferromagnetic metals," *IEEE Trans. Magn.*, vol. 41, no. 10, pp. 3538–3543, Oct. 2005, doi: 10.1109/TMAG.2005.854725.
[31] L. K. Wilson, G. C. Bailey, and C. Vittoria, "Temperature dependence of the parallel magnetic resonance linewidth of permalloy film," in *Proc. AIP Conf.*, vol. 5, p. 1133, 1972, doi: 10.1063/1.2953824.
[32] C. E. Patton, Z. Frait, and C. H. Wilts, "Frequency dependence of the parallel and perpendicular ferromagnetic resonance linewidth in Permalloy films, 2-36 GHz," *J. Appl. Phys.*, vol. 46, no. 11, p. 5002, 1975, doi: 10.1063/1.321489.

MARTINO ALDRIGO (Member, IEEE) received the Ph.D. degree in electronics engineering, telecommunications, and information technology from the Faculty of Engineering, University of Bologna, Italy, in 2014.

Since 2014, he has been a Principal Researcher III with IMT-Bucharest, Romania. His main expertise comprises the electromagnetic simulation and experimental characterization of RF/microwave/millimeter-wave/THz systems for wireless/energy-harvesting applications. He has coauthored more than 60 papers in ISI-ranked journals and conferences. He serves or has served as a Reviewer for many journals and as the Co-Chair in International conferences.

ALINA CISMARU received the master's and Ph.D. degrees in physics from the Physics Faculty, University of Bucharest, in 2000 and 2008, respectively.

Since 2014, she has been a Principal Researcher II with IMT-Bucharest, Romania. Her main expertise is the design and fabrication of EMBG-based devices for microwave applications, CNT-based sensors for the detection of "green-house" type gases (CO, CO2, and CH4), SAW and FBAR characterization for microwave applications, and microphysics characterization using WLI (white-light interferometer). She has coauthored more than 60 scientific papers in ISI-ranked journals and conferences.

MIRCEA DRAGOMAN received the Ph.D. degree in electronics from the University "Politehnica" Bucharest, Romania, in 1991.

He is currently a Senior Researcher I with IMT-Bucharest, Romania. He has coauthored more than 250 scientific papers in ISI ranked journals and conferences, and six monographs.

Prof. Dragoman was a recipient of the Humboldt Fellowship Award and followed postdoctoral studies at Duisburg University, Germany, from 1992 to 1994. He was awarded the "Gheorghe Cartianu" prize of the Romanian Academy in 1999.

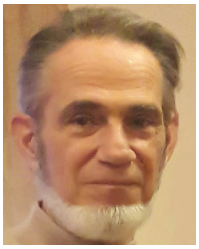

SERGIU IORDANESCU (Life Member, IEEE) received the Ph.D. degree in electronic engineering from the University "Politehnica" Bucharest, Romania, in 2000.

From 1972 to 1977, he was with the Institute of Physics and Technology of Radiation Apparatus, Romania. He was a Research Scientist with IMT-Bucharest, Romania, from 1977 to 2000, and a Senior Engineer with Alvarion Romania SRL, from 2000 to 2015. Since 2015, he has been a Senior Researcher with IMT-Bucharest, Romania. His research interests include microwave SAW filter, sensor and microwave/millimeter-wave circuits design and characterization, as well as dielectric and ferroelectric materials characterization. He is the author of more than 100 scientific papers in peer-reviewed journals and conferences. He received the "Tudor Tanasescu" Romanian Academy Award (with the team) in 2003.

EMANUELA PROIETTI received the degree in electronic engineering, in 1996.

From 1996 to 2000, she worked as the Clean Room Lead Engineer in Texas Instruments Italia, Avezzano Semiconductor Plant. In 2000, she joined the ALCATEL Italia, Rieti plant, as the Maintenance Director for Surface Mount Technology assembly production equipment. In 2001, she joined IMM-Rome as a Research Engineer. From 2005 to 2014, she was the Clean Room Area Coordinator of the IMM-Roma institute. In 2010, she has spent one month in Prof. Peter H. Siegel's Group, CalTech, and JPL, Pasadena, to study the SAR of tissue exposed to low power millimeter radiation. She has served as the coordinator/team member of several national and international projects. Her current scientific interests include RF-MEMS devices, polymeric-based RF devices and membrane, and meta-structured devices for microwave.

GIOVANNI MARIA SARDI (Member, IEEE) was born in Siena, Italy, in 1980. He received the M.Sc. degree in telecommunication engineering and the Ph.D. degrees in information engineering (curricula for electromagnetic waves engineering) from the University of Siena, in 2008 and 2012, respectively.

He is currently a Researcher with the Institute for Microelectronics and Microsystems, National Research Council of Italy, Rome (CNR-IMM). He has published articles in various conferences and journals. His main research topics are design, modeling, and testing of radio-frequency devices for telecommunications and sensing. He is also interested in microwave microscopy applications and applied electromagnetics theory. He serves as a reviewer for journals and as a TPC member in conferences about antennas, microwave devices, and high-frequency sensors. He thanks the Precari Uniti CNR Association for the support in conducting his research activity.

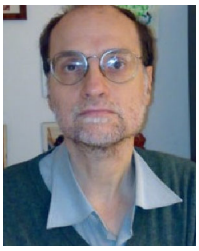

GIANCARLO BARTOLUCCI graduated from the University of Roma La Sapienza, in 1982, with a thesis on integrated optics. In 1982, he was with the "Fondazione Ugo Bordoni," Roma. In 1984, he became a Researcher with the Department of Electronic Engineering, University of Roma "Tor Vergata," where he has been an Associate Professor, since 1992. He has conducted research on the modeling of microstrip and coplanar passive components. His research interests include the development of equivalent circuits for RF MEMS devices and their use for the design of switches and phase shifters. He is also active in the field of metamaterial structures and circuits for high-frequency applications.

ROMOLO MARCELLI (Member, IEEE) was born in Rome, Italy, in 1958. He received the degree in physics from the University of Roma "La Sapienza," in 1983. Since 1987, he has been with the National Research Council (CNR), Italy. Since 1998, he has been with the Institute for Microelectronics and Microsystems (IMM), CNR. He is currently a Senior Researcher at CNR-IMM Roma. He is a member of the IEEE Magnetism and Microwave Theory and Techniques Societies, and the American Physical Society. From 1995 to 1997, he was a member of the Administrative Committee for the IEEE Magnetics Society. He has managed several national and international projects and served as an organizer and committee member in workshops and conferences. He is a referee for several journals in the fields of interest. He has coauthored more than 200 scientific papers in international journals and conferences, and two books. His interests include technologies, design, and test activities in microwave magnetics and RF MEMS, microwave imaging, and metamaterials at microwave and millimeter-wave frequencies.